www.czasopisma.pan.pl PAN www.journals.pan.pl

ARCHIVES of FOUNDRY ENGINEERING

DE GRUYTER OPEN

ISSN (2299-2944)
Volume 16
Issue 4/2016

DOI: 10.1515/afe-2016-0082

Published quarterly as the organ of the Foundry Commission of the Polish Academy of Sciences

47 – 56

Dry Sliding Wear Behavior of Super Duplex Stainless Steel AISI 2507: a Statistical Approach

M. Davanageri [a, *], S. Narendranath [b], R. Kadoli [b]

[a] Department of Mechanical Engineering, Sahyadri College of Engineering and Management, Karnataka, India
[b] Department of Mechanical Engineering, National Institute of Technology Karnataka, Surathkal, India
*Corresponding author. E-mail address: mahesh.mech@sahyadri.edu.in

Received 30.07.2016; accepted in revised form 02.09.2016

Abstract

The dry sliding wear behavior of heat-treated super duplex stainless steel AISI 2507 was examined by taking pin-on-disc type of wear-test rig. Independent parameters, namely applied load, sliding distance, and sliding speed, influence mainly the wear rate of super duplex stainless steel. The said material was heat treated to a temperature of 850°C for 1 hour followed by water quenching. The heat treatment was carried out to precipitate the secondary sigma phase formation. Experiments were conducted to study the influence of independent parameters set at three factor levels using the L_{27} orthogonal array of the Taguchi experimental design on the wear rate. Statistical significance of both individual and combined factor effects was determined for specific wear rate. Surface plots were drawn to explain the behavior of independent variables on the measured wear rate. Statistically, the models were validated using the analysis of variance test. Multiple non-linear regression equations were derived for wear rate expressed as non-linear functions of independent variables. Further, the prediction accuracy of the developed regression equation was tested with the actual experiments. The independent parameters responsible for the desired minimum wear rate were determined by using the desirability function approach. The worn-out surface characteristics obtained for the minimum wear rate was examined using the scanning electron microscope. The desired smooth surface was obtained for the determined optimal condition by desirability function approach.

Keywords: Duplex stainless steel, Specific wear rate, Taguchi method, Response surface methodology, Desirability function approach

1. Introduction

Duplex Stainless Steel (DSS) is characterized by a dual-phase microstructure, comprising almost equal proportions of austenite and ferrite. High mechanical strength combined with better corrosion resistance in aggressive environments has allowed DSS to be used in chemical, petrochemical, oil, nuclear and marine industries [1-5]. The DSS parts also find major applications in paper industry, automobile, aerospace industries [6]. The pumps, valves, and bearings have relative sliding motion (often with self-mated contacts) poses low abrasive and adhesive (galling and seizure) wear resistance [7-8]. In many mechanical applications such as couplings, flanges, bearings, valves, and gears are required to slide against each other in dry conditions at velocity less than 1 m/s [9]. The super duplex cast steel wear behaviour was correlated with the kinetics of sigma phase precipitation by Brodziak-Hyska et al. [2]. The results shown, sigma-phase precipitated between the time intervals of 30-180 min at a temperature of 800 ^{o}C. The σ phase is detected as the secondary

phases at temperature of 850 °C [3]. DSS precipitates secondary phases, when subjected to heat treatment between 550°C and 1000°C and the secondary phases that were precipitated namely chi (χ), secondary austenite (χ_2), sigma (σ), carbides and nitrides [10-16]. The precipitation of sigma phases are generated when exposed to a temperature interval between 700 and 1200 °C. The σ-phase considered being the most influential generated secondary phases as it directly affects the toughness and corrosion behaviour. The inter-metallic R, Π and chi (χ) phase disappears at temperature above 800 °C [10]. The corrosion and erosion behaviour of two cast steels subjected to two different heat treatment temperature and time, which led to the precipitation of σ phase [14]. The volume fractions of carbides, austenite and ferrite predicted through Thermo-Calc software showed consistent results with experimental fractions of the phases obtained in alloy structure [15]. Many research works have reported the effects of heat treatment on the impact of strength, corrosion and microstructure features of DSS [11, 17]. Pressurized fluid flow pipes, tubes, pumps, transmitters, etc. are made of super DSS that wears out quickly. However, their behavior has been neglected in most of the studies. Precipitation of the secondary phase of sigma has been reported to result in a rapid reduction of toughness [18]. The concentration of the phase at high temperature and holding time has substantially reduced the ductility with improved hardness, modulus of elasticity, yield and tensile strength. Authors [19-20] observed a remarkable improvement in tensile strength with a high concentration of secondary phases [19-20], which was attributed either to the precipitation phenomenon or increased ferrite content. Plasma coating, laser surface re-melting, and laser melt injection processes have been reported to improve the wear resistance property of DSS [21-22]. However, small improvements in wear resistance are expected to compensate the need for high cost equipment and its processing. Studies of thermal treatment of wear were conducted for the DSS [23]. The results of these studies showed that the wear resistance increased as a result of the hardness formed by the precipitation of the sigma phase, which enhanced the resistance against the initiated stresses caused by the action of the pin on the surface.

The key observations made from the above literature are listed as follows:

1. The trial and error method of conventional experiments was conducted to enhance the wear resistance property that resulted in local optimal solutions and required conduction of huge experiments.

2. The practical guidelines suggested by many authors to enhance the wear resistance property might not provide detailed information of a process.

3. Significance of individual and interaction factor effects were not statistically estimated.

4. Surface plots graphically explore the wear rate behavior with the independent parameters when they are varied between their respective levels. However, not much work has been reported.

5. Foundry personnel can predict the wear rate for the known set of independent parameters without performing an experiment. However, no studies have conducted a multiple nonlinear regression to derive equations to predict this process.

6. The independent variables responsible for the desired minimum wear rate for practical utility in industries is not yet determined clearly.

The present work investigates the wear behavior of super DSS AISI2507 subjected to heat treatment temperature at 850 °C for 1 hour followed by water quenching. Further, the above observations were addressed to determine the minimum wear rate after conducting a systematic study to provide a complete insight of detailed information of a process.

2. Materials and Experimental Procedures

Experiments were conducted on industrially manufactured and cast super DSS AISI 2507, also referred to as EN 1.4410. The chemical composition of the material was carried on an optical emission spectroscope and its composition is shown in Table 1. The geometrical dimension of the as-cast received material is 10 mm in diameter. The specimen for heat treatment and wear test were prepared as per the ASTM G99A as shown in Fig.1a. The heat treatment conditions were selected based on research work conducted by many authors earlier [11-13]. The specimens were subjected to a solution heat treatment at 1050 °C for 2 hours followed by water quenching to ensure recrystallization of both the phases and the formation of balanced ferrite and austenite microstructure. Further, the heat treatment was carried at a specific temperature of 850 °C for 1 hour followed by water quenching to induce the sigma phase. The optical microscope (ZEISS) and the Scanning Electron Microscope (SEM) (Model: Hitachi Model S-3400N) were used to study the microstructure of the solution-treated and heat-treated specimens. The evaluation of wear characteristics of the heat-treated specimens was carried out by using the dry sliding wear-test rig (Model: DUCOM TR-20) as shown in Fig.1b. The prepared specimens were polished and cleaned with the standard metallographic techniques before conducting the wear test. The specimen weights were measured before and after the wear tests by using a digital weighing balance with an accuracy of 0.1 mg.

Table 1.
Chemical composition of AISI 2507 SDSS (wt. %)

C	Cr	Ni	Mo	Mn	Si	N	Fe
0.019	25.387	6.714	3.77	0.738	0.328	0.028	Bal

The microstructures of solution-treated specimen are shown in Fig.2. The results showed that the strips of austenitic phase and ferritic phase were distributed alternately and approximately in equal proportions during the solution treatment process. The volume fraction of different phase analysis was conducted by using the image analyzer software available in optical microscope according to the ASTM 562 standards. The dual-phase ferrite (δ) and austenite (γ) were observed in the absence of secondary phases. The microstructure of heat-treated specimen at 850 °C is

shown in Fig. 3. The heat treatment results in the precipitation of the secondary sigma phase. The sigma (σ) phase is precipitated in high Cr-concentrated area of (δ) -ferrite and directly forms (δ) -ferrite particles.

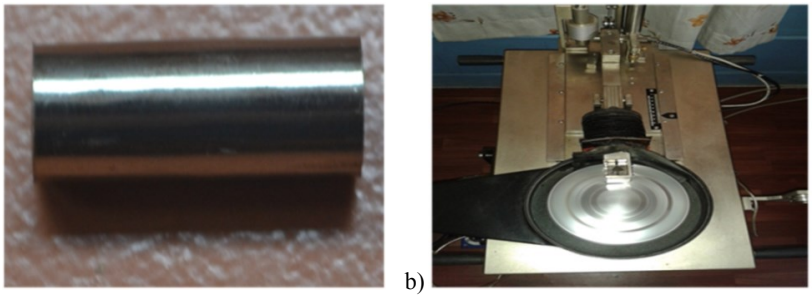

a) b)

Fig. 1. a) Wear test specimen (Pin), and b) Pin on disc type wear test rig

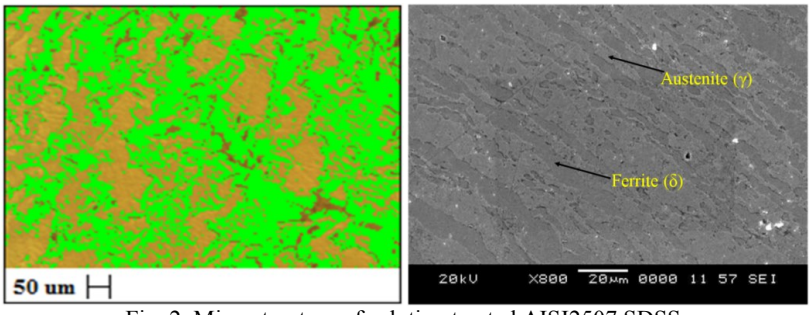

Fig. 2. Microstructure of solution treated AISI2507 SDSS

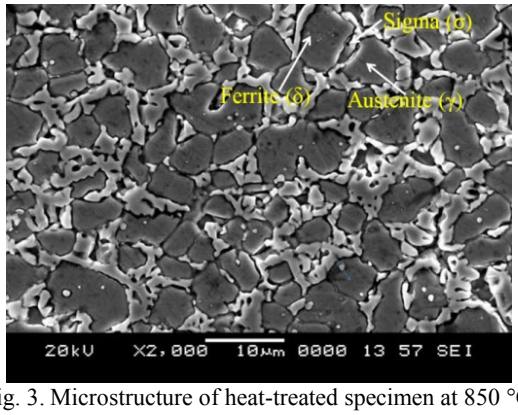

Fig. 3. Microstructure of heat-treated specimen at 850 °C

2.1. Experimental modeling and optimization

The Taguchi method is widely used to collect the experimental input-output data, to analyze the influence of input variable on measured output, which is an unknown function of these process variables, and design high quality systems [24, 25]. The Taguchi method is applied successfully to solve the wear rate behavior of metal matrix composites [26-30]. Response surface methodology is used to study the dry sliding behavior of Al-7075 and Al-7075 hybrid composites [31]. Further, desirability function approach was used to determine minimum wear rate and corresponding input variables [31]. Experiments were conducted according to the standard matrices of L_{27} orthogonal array of the Taguchi method. The input parameters and their corresponding levels influence the specific wear rate and were selected after conducting some pilot experiments and referring past literature [26-30]. The input parameters and the corresponding levels were used for the present work as shown in Table 2. The wear rate was measured for each experimental condition of L_{27} orthogonal array. The collected input-output data were analyzed statistically for input factor significance, by surface plots to establish multiple non-linear regression using response surface methodology (RSM). Statistical significance of the wear rate model was validated by using analysis of variance (ANOVA). The wear rate prediction for the known set of experimental conditions was tested. Further, the set of input parameters responsible for minimum wear rate was determined by using the desirability function approach.

Table 2.
Parameters and their levels

Parameters	Unit	Notation	Levels		
			1	2	3
Load	N	A	20	40	60
Sliding distance	m	B	400	800	1200
Sliding velocity	m/s	C	2	4	6

2.2. Wear test

The pin was pressed against the counterpart of EN32 steel disc having a hardness of 63 HRC to study the wear rate behavior. The wear tests were conducted according to the ASTM G99 standards for each experimental condition of L_{27} orthogonal array. The collected experimental input-output data is shown in Table 3. The pin specimens (heat treated at 850°C for 1 hour) of 10 mm diameter and 30 mm height were made to slide over the counterpart disc. Prior to wear tests, the specimen end face and the counterpart mating surface was polished to an approximate surface roughness value corresponding to 1 µm. This process helped to attain uniform contact between the pin and the counterpart. For each experimental trial, the pin and the disc were cleaned with acetone, dried and the corresponding pin weights were measured using digital weighing balance with an accuracy of 0.1 mg.

3. Results and Discussion

The input-output data were collected according to the Taguchi matrices of L_{27} orthogonal array to investigate the influence of input parameters on the wear rate by using surface plots and significance tests using RSM. The model developed for the wear rate was evaluated using ANOVA. The wear rate prediction accuracy was obtained with experiment values using the derived response equation. Thus, the optimum wear rate responsible for the set of input conditions was determined.

3.1. Statistical Analysis

The output function value is converted to signal to noise (S/N) ratio and is treated as a quality characteristic. Smaller values were considered to possess better quality characteristics required for enhanced properties of wear rate objective function as per Eq. 1.

$$N = -10log\frac{1}{10}\sum_{i=1}^{n} Y_i^2 \tag{1}$$

The S/N ratio value is determined to estimate the main factorial effects on the specific wear rate. Minitab software was used to perform computations and related statistical analysis. The delta value determined for all input factors, based on the computed S/N ratio, is presented in Table 4.

Table 3.
L_{27} Orthogonal array and response table for S/N ratios (smaller is better)

Sl. No.	Load(N)	Sliding distance (m)	Sliding velocity (m/s)	Specific wear rate (mm3/Nm)	S/N ratio [dB]
1	20	400	2	2.100	-6.44439
2	20	400	4	1.885	-5.50623
3	20	400	6	1.700	-4.60898
4	20	800	2	2.010	-6.06392
5	20	800	4	1.870	-5.43683
6	20	800	6	1.656	-4.38121
7	20	1200	2	2.250	-7.04365
8	20	1200	4	2.000	-6.02060
9	20	1200	6	1.890	-5.52924
10	40	400	2	2.125	-6.54718
11	40	400	4	1.906	-5.60246
12	40	400	6	1.798	-5.09579
13	40	800	2	2.560	-8.16480
14	40	800	4	2.350	-7.42136
15	40	800	6	2.220	-6.92706
16	40	1200	2	2.800	-8.94316
17	40	1200	4	2.650	-8.46492
18	40	1200	6	2.529	-8.05898
19	60	400	2	2.880	-9.18785
20	60	400	4	2.720	-8.69138
21	60	400	6	2.660	-8.49763
22	60	800	2	2.990	-9.51342
23	60	800	4	2.770	-8.84960
24	60	800	6	2.591	-8.26935
25	60	1200	2	2.900	-9.24796
26	60	1200	4	2.680	-8.56270
27	60	1200	6	2.540	-8.09667

Table 4.
Main effect values of wear rate for independent parameters

Level	Load (N)	Sliding Distance (m)	Sliding Velocity(m/s)
1	5.671	6.687	7.906
2	7.247	7.225	7.173
3	8.769	7.779	6.607
Delta	3.098	1.087	1.299
Rank	1	3	2

Fig. 4 graphically show the main factorial effects on the measured specific wear rate. The main effect plots were drawn by taking the average output value of an independent parameter set at their respective levels. This refers to the mean response of the factors that varies over the levels. High S/N ratio values always result in producing optimum quality with minimum variance. Fig. 4 shows the main effect values of S/N ratio for wear rate with independent parameters varied between their respective levels. The desired minimum wear rate can be obtained with values of parameter at their respective levels determined as high S/N ratio. Fig. 4 show clearly that the factor combination, set at level 1 of load and sliding distance and at level 3 of sliding velocity, may produce the minimum specific wear rate. This concludes that the minimum specific wear rate lies at low values of sliding distance and applied load and at high values of sliding velocity.

3.2. Surface Plot

Surface plot helps to explain the wear rate behavior with change in independent variables when varied between their respective levels. Surface plots are analyzed by varying two input variables simultaneously, after maintaining the rest at fixed middle values. The following key observations were drawn from the surface plots of wear rate:

1. The wear rate linearly increases with the increase in sliding distance and sliding velocity as shown in Fig.5 (a-b).The applied load contributes more when compared to sliding distance and sliding velocity.
2. Fig.5(c) shows the wear rate behavior with sliding distance and sliding velocity. The resulting surface plot is seen to be almost flat indicating that the sliding distance and the sliding velocity variation between their respective levels does not contribute much towards the wear rate.

The resulting surface plots were almost linear in nature and were consistently in good agreement with the obtained results of significance tests. As the load increases, the penetration ability of the fractured surface results in distinct cut marks with spalling areas that help to remove more material due to the action of pins on the surface [27-28]. Moreover, particles that were worn out and fractured due to the friction left on the contour face of the disc have greater chances of getting locked between the mating pairs, resulting in abrasion and inefficiency to decrease with an increase in sliding distance and sliding velocity [27].

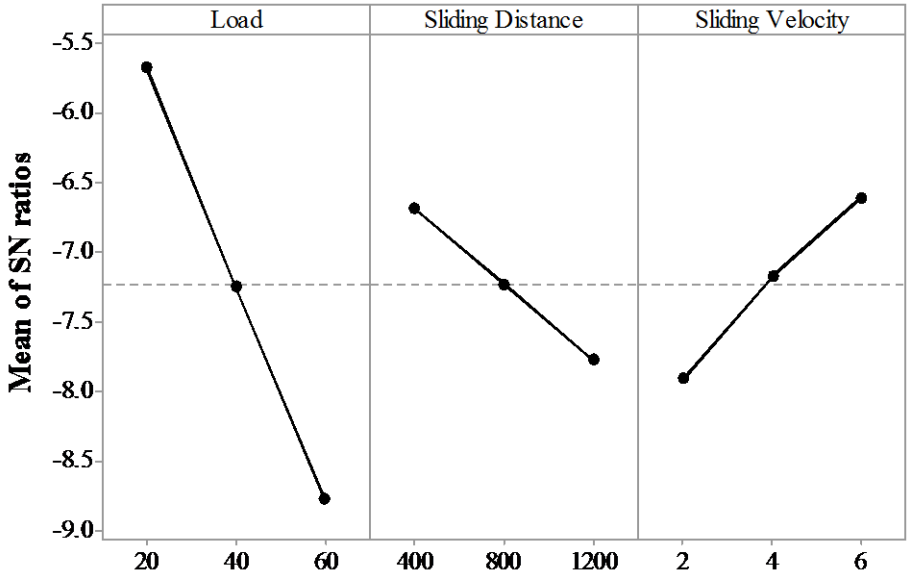

Fig. 4. Main effect plot for S/N ratio of specific wear rate

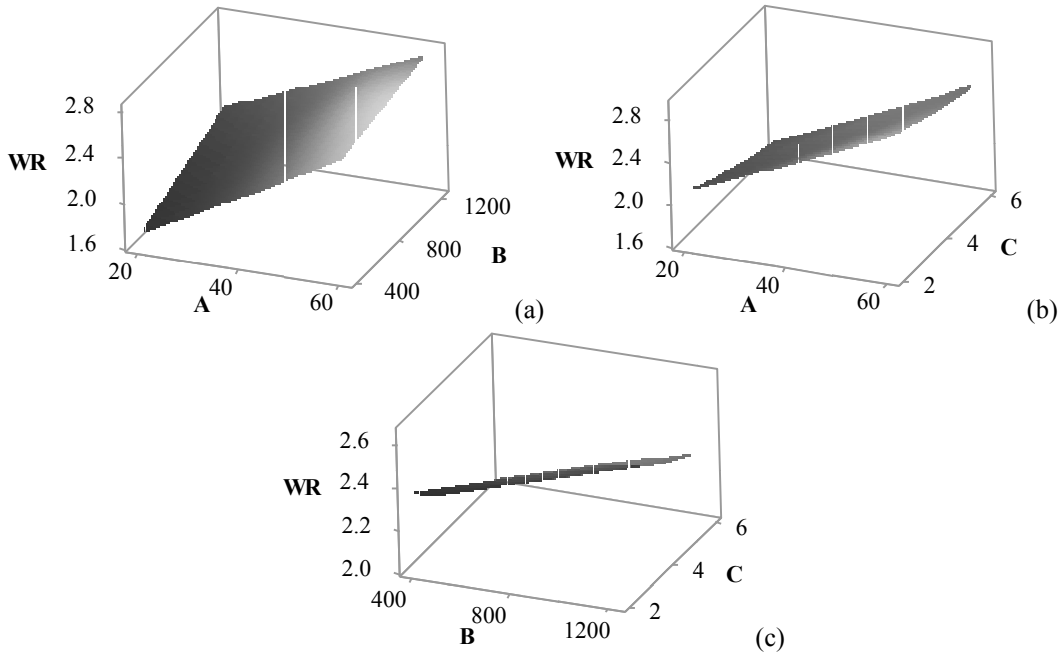

Fig. 5. Surface plots of wear rate with: a) Load and sliding distance, b) load and sliding velocity, and c) sliding distance and sliding velocity

3.3. Analysis of Variance

ANOVA test was conducted to study the statistical significance of individual, quadratic and interactive effects of the factors for specific wear rate. The significant and insignificant terms were determined for the preset 95% confidence level as shown in Table 5. All linear (A, B, C) parameters were found statistically significant for specific wear rate. However, their corresponding square (AA, BB and CC) and interaction (AB, AC and BC) terms were determined insignificant, as the corresponding p-values were found less than 0.05. The applied load followed by sliding velocity and sliding distance showed the highest percent of contribution among all full quadratic terms (refer Table 6). The model validated statistically with good multiple correlation coefficients of 0.885. Thereby, the developed models can be used effectively to test the prediction accuracy of wear rate with experimental cases.

Table 5.
Results of significance tests for specific wear rate

Response	Correlation coefficient		Terms	
	All R terms	Insignificant terms	Significant	Insignificant
Specific Wear Rate, mm3/Nm	0.8850	0.8242	A, B and C	AA, BB, CC, AB, AC, and BC

Table 6.
Test results of ANOVA for wear rate

Source	DF	Adj SS	Adj MS	F	P	% Contribution
Regression	9	3.90295	0.43366	14.54	0.000	88.50
Linear	3	3.86556	1.28852	43.21	0.000	87.66
A	1	3.01761	3.01761	101.19	0.000	68.43
B	1	0.33757	0.33757	11.32	0.004	07.65
C	1	0.51039	0.51039	17.11	0.001	11.57
Square	3	0.00621	0.00207	0.07	0.975	0.14
A^2	1	0.00086	0.00086	0.03	0.867	0.02
B^2	1	0.00001	0.00001	0.00	0.987	0.00
C^2	1	0.00534	0.00534	0.18	0.677	0.12
Interaction	3	0.03118	0.01039	0.35	0.791	0.71
AB	1	0.02952	0.02950	0.99	0.334	0.67
AC	1	0.00152	0.00152	0.05	0.824	0.03
BC	1	0.00016	0.00016	0.01	0.942	0.00
Error	17	0.50696	0.02982			11.50
Total	26	4.40991				100.0

3.4. Multiple non-linear regression analysis

The multiple non-linear regression equation expressed wear rate as a second order polynomial function with input variables as shown in Eq. 2.

$$Specific\ wear\ rate = 1.546 + 0.0219A + 0.00062B - 0.151C - 0.00003A^2 - 0.000000007B^2 + 0.0075C^2 - 0.000006AB + 0.00028AC - 0.000005BC \quad (2)$$

The prediction accuracy of the derived response equation was tested with the experimental values of specific wear rate. The results showed the wear rate varies both on positive and negative sides in the ranges between 9.01% and 13.25% and the average absolute deviation in prediction was found to be equal to 6.89%. Further, the model was also tested for prediction accuracy after removing the insignificant terms from the derived response equation as shown in Eq. 3.

$$Specific\ wear\ rate = 1.546 + 0.0219A + 0.00062B - 0.151C \quad (3)$$

The prediction accuracy was also tested for the same experimental conditions by only considering the significant parameters in the derived response equation as shown in Eq. 3. The deviation in prediction was found to vary on both maximum positive and negative sides in the ranges between 13.86% and 22.0%, and the mean absolute percent deviation was found to be equal to 7.19. This indicates removing non-significant terms that produce large percent deviations from the zero reference line and reduce the prediction accuracy in terms of average absolute percent. Thereby, insignificant terms were not to be removed from the response equation as it reduces the prediction precision (Table 7).

Table 7.
Summary results of prediction of wear rate

Exp. No	A	B	C	WR (mm3/Nm)	Including all terms			Only significant terms		
					Predicted WR	Dev. (%)	Abs. Dev. (%)	Predicted WR	Dev. (%)	Abs. Dev. (%)
1	20	400	2	2.100	1.906	9.23	9.23	1.930	8.10	8.10
2	20	400	4	1.885	1.701	9.75	9.75	1.628	13.63	13.63
3	20	400	6	1.700	1.556	8.44	8.44	1.326	22.00	22.00
4	20	800	2	2.010	2.099	-4.41	4.41	2.178	-8.36	8.36
5	20	800	4	1.870	1.890	-1.07	1.07	1.876	-0.32	0.32
6	20	800	6	1.656	1.741	-5.14	5.14	1.574	4.95	4.95
7	20	1200	2	2.250	2.289	-1.74	1.74	2.426	-7.82	7.82
8	20	1200	4	2.000	2.076	-3.82	3.82	2.124	-6.20	6.20
9	20	1200	6	1.890	1.924	-1.77	1.77	1.822	3.60	3.60
10	40	400	2	2.125	2.271	-6.88	6.88	2.368	-11.44	11.44
11	40	400	4	1.906	2.078	-9.01	9.01	2.066	-8.39	8.39
12	40	400	6	1.798	1.944	-8.12	8.12	1.764	1.89	1.89
13	40	800	2	2.560	2.416	5.63	5.63	2.616	-2.19	2.19
14	40	800	4	2.350	2.218	5.60	5.60	2.314	1.53	1.53
15	40	800	6	2.220	2.081	6.27	6.27	2.012	9.37	9.37
16	40	1200	2	2.800	2.558	8.63	8.63	2.864	-2.29	2.29
17	40	1200	4	2.650	2.357	11.07	11.07	2.562	3.32	3.32
18	40	1200	6	2.529	2.215	12.41	12.41	2.260	10.64	10.64
19	60	400	2	2.880	2.612	9.29	9.29	2.806	2.57	2.57
20	60	400	4	2.720	2.430	10.66	10.66	2.504	7.94	7.94
21	60	400	6	2.660	2.308	13.25	13.25	2.202	17.22	17.22
22	60	800	2	2.990	2.709	9.39	9.39	3.054	-2.14	2.14
23	60	800	4	2.770	2.523	8.93	8.93	2.752	0.65	0.65
24	60	800	6	2.591	2.396	7.51	7.51	2.450	5.44	5.44
25	60	1200	2	2.900	2.804	3.33	3.33	3.302	-13.86	13.86
26	60	1200	4	2.680	2.613	2.50	2.50	3.000	-11.94	11.94
27	60	1200	6	2.540	2.483	2.26	2.26	2.698	-6.22	6.22

The residuals were distributed normally along the straight line for wear rate as shown in the probability plot in Fig. 6. The effects were negligible and were normally distributed, with a mean zero and a variance σ^2. Normal probability plot is a graphical technique that uses the basic concept of central limit theorem. The points close to the fitted line, especially towards the middle group, represent the estimated factors which do not show major significance on output variable.

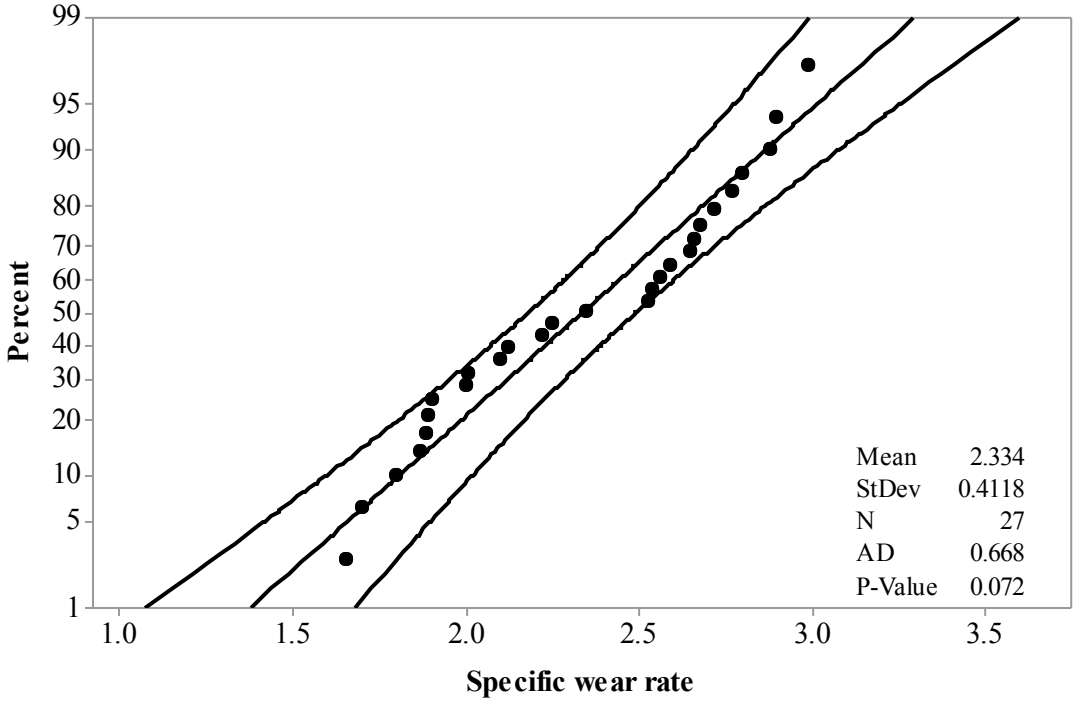

Fig. 6. Normal probability plot for specific wear rate

3.5. Optimization

The pressurized fluid flow through pipes, tubes, pumps, transmitters, etc. require better wear resistance characteristics. The input parameters that yield the desired minimum wear rate are of industrial relevance. Desirability function approach was used to achieve the desired wear resistance. In DFA, the objective function value is converted to desirability function value, which usually varies in the ranges between 0 and 1 ($0 \leq d_i \leq 1$). Zero value representing the objective function is completely undesirable, whereas one denoting the ideal is a desirable value. The desirability value for the minimization type of objective function is determined as shown in Eq. 4.

$$Y_{WR} = \frac{WR_{max} - WR}{WR_{max} - WR_{min}} \tag{4}$$

Where, WR_{max} is the maximum value of specific wear rate, and WR_{min} is the minimum value of specific wear rate.

The desired optimized combination of input variables determined for the minimum wear rate using the desirability function approach is shown in Table 8. The desirability function approach determines the minimum wear rate with the highest desirability value equal to 1. It is important to note that the desired minimum wear rate was obtained using the desirability function approach as it is one of the combinations of 27 different experiments conducted. The microstructure characterization, by using the SEM on the worn-out surface of AISI 2507 super DSS, is obtained for the desired minimum wear rate as shown in Table 8. The applied load on the hard roughness of the parent metal tends to plough the surface due to the action of pins resulting in a smooth surface with mild grooves on the worn-out material as shown in Fig. 7. Increase in load and sliding distance causes severe plastic deformation, which in turn leads to parallel deep groove formation with the debris of wear spread all over the worn-out surface as shown in Fig. 7. High stress concentration during sliding at high load tends to initiate cracks which penetrate in parallel to the sliding direction. Thus, the debris formed with action of pin surface creates parallel and deeper ploughs as shown in Fig. 7. Similar trend observations were found in earlier literature [15-17].

Table 8.
Specific wear rate and corresponding optimization set of input parameters

Sl. No	Decision variables			Output
	Load, N	Sliding distance, m	Sliding velocity, m/s	Specific wear rate, mm3/Nm
1	20	400	6	1.5761

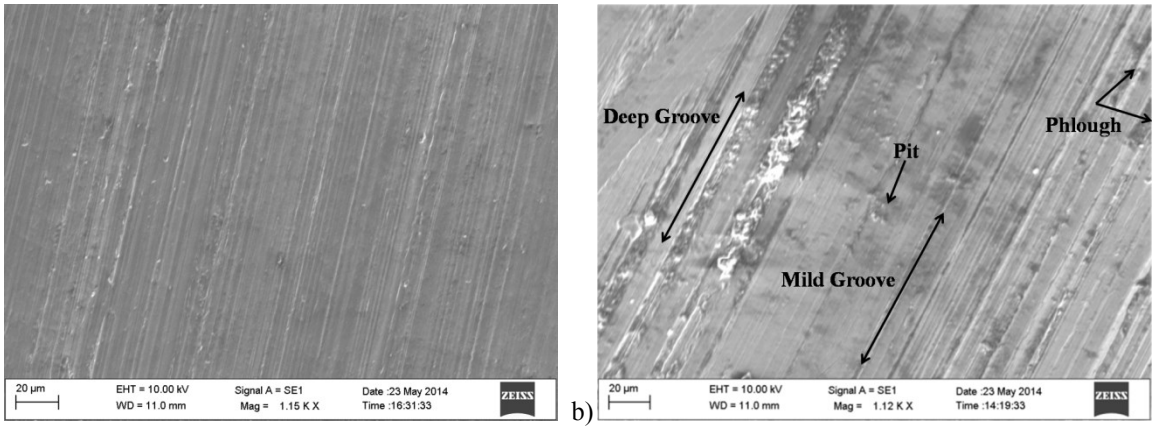

Fig. 7. SEM micrographs of worn-out surface for different input conditions: a) Optimized input conditions (A=20, B=400, and C=6) obtained minimum WR and b) Input conditions (A=60, B=800, and C=2) determined high WR

4. Conclusions

Experiments were conducted according to the design matrices of L_{27} orthogonal array of the Taguchi method. Surface plots, ANOVA, significance tests, and mathematical input-output relationships were derived using RSM. The developed wear rate equations were tested for prediction accuracy with 27 experimental conditions. Further, the optimum input parameters responsible for the desired minimum wear rate were performed using the desirability function approach. The following key observations were made from the obtained wear rate results of heat-treated super DSS:

1. The desired secondary sigma phase was obtained for the specimen heat treated at 1050 °C for 2 hours followed by water quenching, and further heat treated at 850 °C for 1 hour.

2. All linear factors were statistically significant for the wear rate. However, the applied load was found to have a major significance, followed by sliding velocity and sliding distance. All factors (load, sliding speed and sliding distance) were found to have a linear relationship with the wear rate, as their corresponding p-values of square terms were greater than 0.05. The interaction factors were not found significant due to the strong linear relationship among all independent parameters.

3. The statistical significance test results were in good agreement with the obtained surface plots. The developed wear rate model is statistically validated using ANOVA with good multiple correlation coefficient.

4. The developed model predicted the specific wear rate with an average absolute percent deviation of 6.89. The non-contributing terms should not be removed from the derived predictive equation as it reduces the prediction accuracy with maximum positive and negative deviations.

5. The desired minimum wear rate obtained from the optimized input conditions of the desirability function approach resulted in an uniformly smooth surface with mild grooves.

6. The developed model is more useful for foundry personnel, industrial applications (pump valves, tubes, pipes and transmitters) and any novice user to obtain the minimum wear rate without conducting practical experiments.

References

[1] Femenia, M., Pan, J., Leygraf, C. & Luukkonen, P. (2001). In situ of selective dissolution of duplex stainless steel 2205 by electrochemical scanning tunnelling microscopy. *Corrosion Science*. 43, 1939-1951.

[2] Brodziak-Hyska, A., Stradomski, Z. & Kolan, C. (2014). Kinetics of the σ phase precipitation in respect of erosion-corrosion wear of duplex cast steel. *Archives of Foundry Engineering*. 14(1), 17-20.

[3] Antony, P.J., Singh Raman, R.K., Mohanram, R., Kumar, P. & Raman, R. (2008). Influence of thermal aging on sulfate-reducing bacteria (SRB)-influenced corrosion behavior of 2205 duplex stainless steel. *Corrosion Science*. 50, 1858-1864.

[4] Eriksson, H. & Bernhardsson, S. (1991). The applicability of duplex stainless steels in sour environments. *Corrosion Science*. 47, 719-725.

[5] Oredsson, J. & Bernhardsson, S. (1983). Performance of high alloy austenitic and duplex stainless steels in sour gas and oil environments. *Material Performance*. 22, 35-42.

[6] Heitkemper, M., Fischer, A., Bohne, C. & Pyzalla, A. (2001). Wear mechanisms of laser-hardened martensitic high-nitrogen-steels under sliding wear. *Wear*. 250(1), 477-484.

[7] Totik, Y., Sadeler, R., Altun, H. & Gavgali, M. (2003). The effects of induction hardening on wear properties of AISI

4140 steel in dry sliding conditions. *Materials and Design*. 24, 25-30.
[8] Boromei, I., Ceschini, L., Marconi, A. & Martini, C. (2003). A duplex treatment to improve the sliding behavior of AISI 316L: Low-temperature carburizing with a DLC (aC: H) topcoat. *Wear*. 302(1), 899-908.
[9] Williams, J.A. (1999). Wear modelling: analytical, computational and mapping: a continuum mechanics approach. *Wear*. *225*, 1-17.
[10] Nilsson, J.O. & Wilson, A. (1993). Influence of isothermal phase transformation on toughness and pitting corrosion of super duplex stainless steel SAF 2507. *Material Science Technology*. 9, 545-554.
[11] Nilsson, J.O. (1992). Super duplex stainless steel. *Material Science Technology*. 8, 685-700.
[12] Chen, T.H. & Yang, J.R. (2001). Effects of solution treatment and continuous cooling onr-phase precipitation in a 2205 duplex stainless steel. *Material Science Engineering A*, 311, 28-41.
[13] Chen, T.H., Weng, K.L. & Yang, J.R. (2002). The effect of high-temperature exposure on the microstructural stability and toughness property in a 2205 duplex stainless steel. *Material Science Engineering A*. 338, 259-270.
[14] Stradomski, Z., Brodziak-Hyska, A. & Kolan, C. (2012). Optimization of sigma phase precipitates with respect to the functional properties of duplex cast steel. *Archives of Foundry Engineering*. 12(2), 75-78.
[15] Stradomski, Z. & Dyja, D. (2007). Characterization of solidification and solid state transformation in duplex cast steel: Thermo-Calc investigation. *Archives of Foundry Engineering*. 7(3), 269-272.
[16] Duprez, L., Cooman, B.D. & Akdut, N. (2000). Microstructure evolution during isothermal annealing of a standard duplex stainless steel type 1.4462. *Steel research*. 71, 417-422.
[17] Lasebikan, B.A., Akisanya, A.R. & Deans, W.F. (2013). The Mechanical Behavior of a 25Cr Super duplex stainless steel at elevated temperature. *Journal of Materials Engineering and Performance*. 22(2), 598-606.
[18] Pohl, M., Storz, O. & Glogowski, T. (2007). Effect of intermetallic precipitations on the properties of duplex stainless steel. *Materials Characterization*. 58, 65-71.
[19] Akisanya, A.R., Obi, U. & Renton, N.C. (2012). Effect of ageing on phase evolution and mechanical properties of a high tungsten super-duplex stainless steel. *Material Science Engineering A*. 535, 281-289.
[20] Badji, R., Bouabdallah, M., Bacroix, B., Kahloun, C., Belkessa, B. & Maza, H. (2008). Phase transformation and mechanical behavior in annealed 2205 duplex stainless steel welds. *Materials Characterization*. 59, 447-453.
[21] Do Nascimento, M., Ocelík, V., Ierardi, M.C.F. & De Hosson, J.T.M. (2008). Wear resistance of WCp/Duplex Stainless Steel metal matrix composite layers prepared by laser melt injection. *Surface Coatings Technology*. 202, 4758-4765.
[22] Martins, M. & Castelleti, L.C. (2005). Effect of heat treatment on the mechanical properties of ASTM A890 Gr6A super duplex stainless steel. *Journal of ASTM International*. 2, 1-14.
[23] Fargas, G., Mestra, M., Anglada, M. (2009). Effect of thermal treatments on the wear behaviour of duplex stainless steels. IOP Conf. Series. Material Science and Engineering A, 5(5).
[24] Roy, K.R. (1990). *A Primer on the Taguchi Method*. New York: Van Nostrand Reinhold.
[25] Ross, P.J. (1993). *Taguchi Technique for Quality Engineering*. New York: McGraw-Hill.
[26] Basavarajappa, S., Chandramohan, G. & Paulo Davim, J. (2007). Application of Taguchi techniques to study dry sliding wear behaviour of metal matrix composites. *Material Design*. 28, 1393-1398.
[27] Mahapatra, Patnaik. (2009). A Study on mechanical and erosion wear behaviour of hybrid composites using Taguchi experimental design. *Material & Design*. 30, 791-801.
[28] Sahoo, P. (2009). Wear behaviour of electroless Ni–P coatings and optimization of process parameters using Taguchi method, *Material Design*. 30, 1341-1349.
[29] Sahin, Y. (2003). Wear behaviour of aluminium alloy and its composites reinforced by SiC particles using statistical analysis. *Materials & Design*. 24(2), 95-103.
[30] Basavarajappa, S. & Chandramohan, G. (2005). Wear Studies on Metal Matrix Composites: a Taguchi Approach. *Journal of Material Science and Technology*. 21(6), 845-850.
[31] Kumar, R. & Dhiman, S. (2013). A study of sliding wear behaviors of Al-7075 alloy and Al-7075 hybrid composite by response surface methodology analysis. *Materials & Design*. 50, 351-359.